# Photoswitchable bactericidal effects from novel silica-coated silver nanoparticles

Gustavo Fuertes[a], Esteban Pedrueza[b], Kamal Abderrafi[b], Rafael Abargues[b], Orlando Sánchez[a], Juan Martínez-Pastor[b], Jesús Salgado[a,c] and Ernesto Jiménez[b,*]
[a]Instituto de Ciencia Molecular and [b]Instituto de Ciencia de Materiales, Universitat de València. 46980 Paterna (Valencia) Spain. [c]Departamento de Bioquímica y Biología Molecular, Universitat de València. 46100 Burjassot (Valencia) Spain.

## ABSTRACT

The enhancement of the electromagnetic field in the surroundings of nanoparticles via surface plasmon resonance offers promising possibilities for biomedical applications. Here we report on the selective triggering of antibacterial activity using a new type of silver nanoparticles coated with silica, Ag@silica, irradiated at their surface plasmon frequency. The nanoparticles are able to bind readily to the surface of bacterial cells, although this does not affect bacterial growing since the silica shell largely attenuates the intrinsic toxicity of silver. However, upon simultaneous exposure to light corresponding to the absorption band of the nanoparticles, bacterial death is triggered selectively on the irradiated zone. Because of the low power density used in the treatments, we discard thermal effects as the cause of cell killing. Instead, we propose that the switched toxicity is due to the enhanced electromagnetic field in the proximity of the nanoparticles, which either directly (through membrane perturbation) or indirectly (through induced photochemical reactions) is able to cause cell death.

Keywords: *Antibacterial, Silver nanoparticles, Core-shell nanoparticles, Silver toxicity, Oxidative etching, Membrane perturbation, Optoporation, Reactive oxygen species*.

*ernesto.jimenez@uv.es;

Medical Laser Applications and Laser-Tissue Interactions V, edited by Ronald Sroka, Lothar D. Lilge, Proc. of SPIE-OSA Biomedical Optics, SPIE Vol. 8092, 80921M

# 1. INTRODUCTION

Materials with dimensions in the nanometer scale present important changes in their physico-chemical properties being the origin of new phenomena with potential technological and biomedical applications [1,2]. However, studies focusing on the biological activity of nanomaterials are still in its infancy. Recent investigations of nanoparticles (NP[1]) report on their antimicrobial activity as well as the enhanced bioactivity of drugs [3-7]. Silver, a metal often employed for the preparation of NP, has been used for centuries as an antibacterial agent. Silver salts such as silver nitrate, silver lactate and silver sulfadiazine have been employed to prevent bacterial infection, like in burn treatments [8-10], in the formulation of dental resin composites or as coatings of medical devices [11-13]. However, the exact action mechanism of silver as a bactericidal is not yet fully understood [14,15]. Silver ions are known to react with sulfhydrils and other chelating groups of proteins, which render these molecules inactive [16]. They also seem to increase the permeability of lipid membranes, making the proton motive force collapse and leading eventually to cell death [17]. These general features should be greatly improved in silver NP due to their large surface area and high reactivity compared to the bulk solid [18]. Indeed, the antibiotic effect of silver NP has already been reported [3,4,19,20], with successful applications as effective antimicrobial coatings for protecting medical devices or in water sanitization filters [21,22]. It is also possible to control the antimicrobial activity of nanosilver in $Ag/TiO_2$ particles by ultraviolet (UV) light irradiation [23].

Outside the biomedical arena, silver NP encounter basic applications in the field of biophysics, being used for single-molecule detection through surface-enhanced Raman scattering (SERS) [24]. Discovered in the late 70s, SERS causes a huge increment in Raman scattering near the metal NP [25,26]. The effect was originally interpreted in terms of an electromagnetic resonance produced in the nanostructure of noble metals [27], which paved the way for the electromagnetic theory of SERS [28]. Nowadays, it is named Surface Plasmon Resonance (SPR) and involves a wide variety of phenomena and applications in diverse fields like biophysics, biomedicine and technology. Examples of successful uses of SPR can be found in biosensing [29], photodynamic and photothermal therapy [30], and lines of optical transmission based on NP [31]. These applications rely on the high electromagnetic fields produced in the vicinity of metal NP because of the polarization of an external electromagnetic field [28]. The enhancement of the local field depends on the shape, size, configuration and composition of the NP [32-34]. For example, at the surface of a resonantly excited isolated NP the increase of field intensity is estimated to be 30-fold, but the multiplication factor can be as large as 5,000 at intermediate *hot* points between coupled NP [34]. Therefore, although such an electromagnetic field decays rapidly with distance to the NP surface [28,34], in its immediate proximity (up to a few nanometers) the excitation light intensity (proportional to the square of the electromagnetic field intensity) can be amplified between $10^3$ and $10^7$ times [34,33,35].

Another important phenomenon is the change in chemical activity of the NP under irradiation with light. For example, laser irradiation of metal NP dispersed in aqueous solutions can lead to either breaking up or fusion of the colloid [36-38]. Moreover, irradiation may also induce the photo ejection of electrons, causing oxidation/ionization at the NP surface and segregation of metal cations [36]. This effect is intensified in the presence of chloride anions due to an $O_2/Cl^-$ oxidative attack known as *oxidative etching*, which in the case of NP with twinned morphology may lead ultimately to complete dissolution [39,40]. The oxidative etching effect has been used for the photoconversion of nanospheres into other different shapes [41,42].

With the above ideas in mind, we aimed to investigate the effect of a new type of silver NP [43,44], including the associated SPR phenomena, on the growing ability of *Escherichia coli* cells. The NP are composed of a silver core and a thin shell (1-2nm) of silica glass, and are hereafter referred to as Ag@silica. Upon proper irradiation, such a tiny silica layer is expected to still allow the induction of enhanced electromagnetic fields over the insulating NP surface. In addition, this coating can diminish the background segregation of $Ag^+$ ions, and thus the associated toxic effects, although still maintaining some porosity which may allow the exchange of ions possibly originated from photo-oxidation induced by light irradiation. In this way, the nanoparticle toxicity could be controlled through laser irradiation in selected sample regions.

1 Abbreviations used: NP, nanoparticle(s); Ag@silica, silica-coated silver NP; SERS, surface enhanced raman scattering; SPR, surface plasmon resonance; UV-Vis, ultraviolet-visible; XRD, X-ray diffraction; TEM, transmission electron microscopy; HRTEM, high resolution TEM; EDX, energy dispersive X-ray spectrometry; SEM, scanning electron microscope; OD600, optical density at 600 nm; ROS, reactive oxygen species; lysogeny broth (LB).

## 2. METHODOLOGY

### 2.1 Preparation and characterization of silica-coated silver nanoparticles

For the synthesis of silver NP coated with silica we used a novel method consisting on the ablation with laser of a high purity (99.99%) silicon target immersed in an aqueous solution of $AgNO_3$ (at 125 μM concentration) [43,44]. The target was irradiated for 264 s using the 3rd harmonic of a Nd:YAG laser (λ=355 nm) with a repetition frequency of 5 kHz and a mean power of 1 W. Large silicon particles produced by splashing during irradiation were removed by filtration with a 200 nm cutoff polyethersulfone membrane (Nalgene®), and stock suspensions of Ag@silica NP were prepared in water at a concentration of ~11 nM, corresponding to $65x10^{14}$ NP $L^{-1}$.

The ultraviolet-visible (UV-Vis) absorption of the NP colloidal solution was recorded using a Shimadzu 2501 spectrophotometer. The structure of the NP was analyzed by X-ray diffraction (XRD) on a Saifert XR3003TT.[44] The shape and size of the NP were examined by transmission electron microscopy (TEM) using a Jeol 1200EX microscope operating at 100 kV. High resolution (HR) TEM images were obtained in a FEI-Tecnai G2 microscope. The composition of NP was studied by energy dispersive X-ray spectrometry (EDX) microanalysis with the help of a Hitachi S-4100 scanning electron microscope (SEM).[44]

### 2.2 Biological assays

Assays of biological activity consisted on the study of effects on the growing ability of *E. coli* bacteria. The laboratory strain BL21(DE3) was used. Experiments conducted on cell suspensions, were made at 37ºC in standard lysogeny broth (LB) medium (10 g $L^{-1}$ tryptone, 5 g $L^{-1}$ yeast extract, 10 g $L^{-1}$ NaCl). The binding of Ag@silica NP to *E. coli* cells was investigated by TEM. The bactericidal effect of Ag@silica NP was tested by adding a suspension of the NP at the beginning of the bacterial growth, and monitoring cell growing through the evolution of the optical density at 600 nm (OD600) at constant temperature. The values of OD600 are proportional to the concentration of cells (OD600=0.1 corresponds approximately to a concentration of $4x10^8$ cells per mL). To test effects of laser irradiation, cells grown in an Erlenmeyer flask until the stationary phase were used to inoculate fresh LB in a 50 μL quartz cell, where they grew while being constantly irradiated by the laser beam. Two experiments were always run in parallel.

The experiments in solid media were conducted in Petri dishes containing LB with 2% agar and supplemented with a suspension of NP. A preculture of bacteria grown in liquid LB as described before, with or without Ag@silica NP, was spread over the plates and incubated overnight with or without continuous laser irradiation in a central spot in the plate. The concentration of cells was adjusted to achieve an almost full coverage of the plate once the colonies were developed.

Two lasers were used for the irradiation of cultures: a semiconductor diode pulsed laser (Edinburgh Instruments) with a wavelength of 405 nm and a bandwidth of 10 nm (blue laser) and a continuous wave He-Ne laser irradiating at 633 nm (red laser). With the blue laser we applied pulses of 100 ps, with a repetition frequency of 20 MHz and a mean power of 0.25 mW, having the laser spot an area of about 1.4 $mm^2$. The red laser irradiated with a power of 5 mW and a spot of 1 $mm^2$. The mean power densities used for the blue and red lasers were 18 mW $cm^{-2}$ and 160 mW $cm^{-2}$, respectively.

## 3. RESULTS

### 3.1 Synthesis and physical characterization of Ag@silica NP

The Ag@silica NP were synthesized in just one step by laser ablation of a highly pure silicon target immersed in an aqueous solution of silver nitrate. This is a new method for preparing surface-covered metal NP and can in principle be used for a variety of dielectric coatings. The final composition of the NP depends on the ratio between the metallic salts diluted in the synthesis solution and the coating molecules, and is determined by the selected target and laser ablation parameters [43,44]. During the synthesis process large silicon particles are formed because of splashing, i.e. the fragmentation of the irradiated surface by the sound wave generated after laser ablation, which are removed by centrifugation or filtration.

Ag@silica NP were characterized by a number of physical techniques. Figure 1A shows the absorption spectra of a suspension of silver NP, with a fairly symmetric band associated to the SPR of silver centered at ~400 nm. In HRTEM images (figure 1B) we observe spherical silver particles with a mean diameter of 11 nm (figure 1A, inset), each one coated with a layer of silica 1-2 nm thick. Twin planes can be distinguished in the silver core (white arrows in figure 1B), along with the twin faces or folds, shaping a decahedric morphology known as twinned morphology. This type of structure is made of 5 tetrahedric mono crystals radially oriented towards a central abscissa, so that all tetrahedra have a corner in common and each one possess two faces in contact with its neighbours. Analyses of XRD data indicate that the silver is present in the form of crystals. However, the characteristic peaks of silica are not observed in the XRD spectra, suggesting that this covering material is amorphous. EDX-SEM measurements from Ag@silica NP show a Si/O ratio of 0.5, again in agreement with the presence of amorphous silica coating [43,44]. This shell is most likely forming a layer of very small silica NP of 1-2 nm diameter (the thickness of the layer), which may leave tiny pores between the packed spheres.

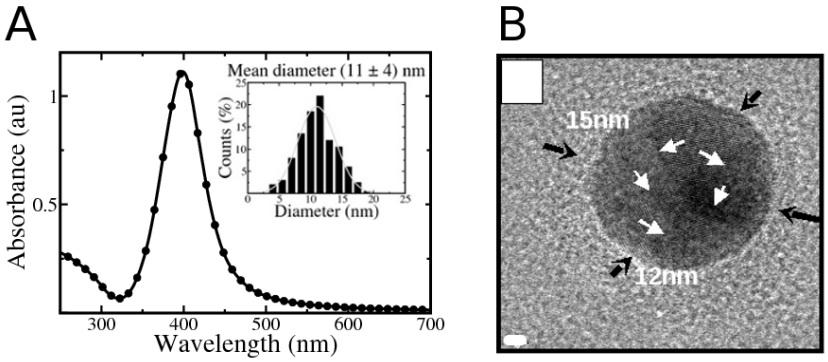


**Figure 1.** Physical characterization of Ag@silica NP: (A) Absorption spectra of a suspension of Ag@silica NP with the Plasmon peak centered at 400 nm. Inset: distribution of particle sizes measured by TEM. The average diameter is 11 nm. (B) HRTEM image of a Ag@silica NP showing the coating of amorphous silica (1-2 nm thick, black arrows) and some visible twin planes (white arrows). Scale bar, 2 nm.

### 3.2 Ag|@silica NP bind readily to the surface of *E. coli* cells

The interaction between Ag@silica NP and *E. coli* cells was investigated by TEM. Ag@silica NP added at a concentration of $0.65 \times 10^{14}$ NP $L^{-1}$ over a fresh growing suspension of *E. coli* are found to accumulate at the cell surface (figure 2A). However, the size of these particles is clearly larger (50-200 nm) than that of the isolated Ag@silica NP, indicating that theyare made of aggregates. This possibility was further supported by absorbance spectra of the Ag@silica NP suspensions in the presence of the *E. coli* bacteria (figure 2B), which clearly show a widening of the characteristic NP absorption band. The spectrum is modified immediately after bacterial addition to the NP and did not change significantly within several hours. These results show that Ag@silica bind readily to the *E. coli* surface, most likely to polysaccharides of the capsule or to lipopolysaccharides or proteins exposed at the external side of the outer lipid membrane, and suggest that such an interaction induces NP clusterization.

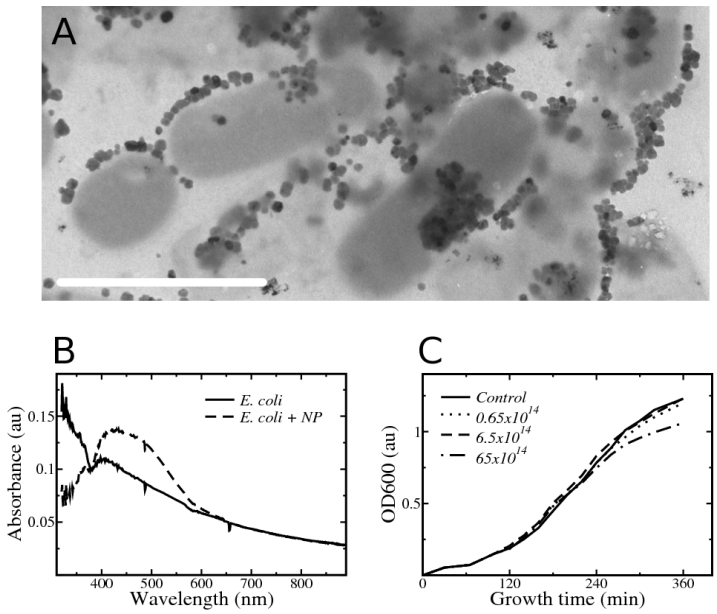


**Figure 2.** Interaction between Ag@silica NP and *E. coli* bacteria. (A) TEM image of a suspension of *E. coli* cells with Ag@silica NP added at a concentration of $0.65x10^{14}$ NP $L^{-1}$. Scale bar, 2 μm. (B) Absorption spectra of a suspension of *E. coli* growing in LB medium before (dotted line) and after addition of Ag@silica NP at a concentration of $6.5x10^{14}$ NP $L^{-1}$(solid line). (C) *E. coli* growing curves followed as the variation of the cell density measured as the OD600 versus time. The concentrations of Ag@silica (given in NP per mL) are shown in the figure legend.

### *3.3* Background activity of Ag@silica against *E. coli*

As it has been described in the introduction, silver NP possesses intrinsic antibiotic activity. However, in our specific case the silica layer is expected to insulate and stabilize the silver core, attenuating or inhibiting the background bactericidal effect. We tested such a possibility by studying the growth of *E. coli* in the presence of Ag@silica NP. The NP were added at the lag phase of the bacterial growth, just before the exponential phase, at concentrations between $0.65x10^{14}$ and $65x10^{14}$ NP $L^{-1}$. The growth curves under these conditions, measured as the OD600 with increasing time, are represented in figure 2C. Only for the largest concentration of Ag@silica NP ($65x10^{14}$ NP $L^{-1}$) we observed a weak toxic effect, which shows as a small reduction in the growing rate. Similar studies performed with uncovered silver NP at comparable concentrations showed much stronger bactericidal effects [3,19]. For example, for non coated silver NP at concentrations of 10 μg $cm^{-3}$ and 20 μg $cm^{-3}$ ,Sondi and Salopeck-Sondi report attenuations of bacterial growth of 70% and 96%, respectively [3]. Being the diameter of their NP 12.3 nm, the latter quantities correspond to $9.7x10^{14}$ NP $L^{-1}$ and $19x10^{14}$ NP $L^{-1}$, respectively [19]. Other investigations using 40 nm silver NP show that the amount of silver needed to cause 90% reduction of growing is about 60 μg $cm^{-3}$, which is equivalent to $1.7x10^{14}$ NP $L^{-1}$. Because of the smaller size of our NP, compared to the latter examples, we would expect a larger effective area in our case, and thus a larger toxicity at similar concentration, but the fact that this is not the case illustrates the protective action of the silica shell.

In summary, our Ag@silica NP have a very small intrinsic inhibitory effect on the growth of *E. coli* suspension cultures, compared to uncovered silver NP. Furthermore, as the Ag@silica NP bind readily to the surface of bacteria (see above and figure 2A), the reduction of the intrinsic silver toxicity is not due to a lack of bacterial proximity, but most likely a consequence of the silica coating.

### 3.4 Triggering bactericidal activity through irradiation at the SPR wavelength.

Next we studied the effect of Ag@silica NP on *E. coli* cultures under conditions of light irradiation. For that we treated bacterial cultures using either of two lasers, blue or red. The wavelength of the blue laser (405 nm) approaches closely to the absorption maximum of the NP spectrum (figures 1A and 2B). The red laser, however, has a wavelength of 633 nm, and was chosen as a negative control since its absorption by the NP is vanishingly small, even after the SPR band widens in the presence of bacteria (figure 2B). A group of experiments was performed in liquid cultures, in which bacteria were

grown in 50 µL spectrophotometer quartz cells, and were irradiated.with the lasers inside a box thermostatted at 37 ºC Figure 3 shows typical growth curves measured under the above conditions. This setup allowed easy measurement of the OD600 in small culture volumes, which are required to achieve a significant irradiation with laser spots of about 1.4 $mm^2$. Thus, for a 3 mm path-length, the irradiated volume is 4.2 µL, which is 9.3% of the total 45 µL culture.. In the cultures with added Ag@silica NP we used a concentration of $6.5x10^{14}$ NP $L^{-1}$ (~3200 NP per bacterial cell at the moment of addition), which is well below the concentration causing measurable intrinsic silver toxicity (figure 2C), allowing the observation of effects on bacterial growth due only to laser irradiation. Samples containing Ag@silica NP and irradiated with the blue laser (figure 3A, filled circles) showed a attenuated growth, with a decrease in the OD600 at the top of the curve between 30% and 40%, compared with control experiments using the same samples without irradiation (figure 3A, empty circles), or samples without NP irradiated with the same laser (figure 3A, filled squares). On the other hand, control experiments made by irradiating with the red laser, either with (figure 3B, filled circles) or without added Ag@silica NP (figure 3B, filled squares), did not show consistent changes in the bacterial growth. These results tell us that the Ag@silica NP must be present for the irradiation to affect the *E. coli* growth, and that the observed effect is specific of a wavelength within the plasmon absorption band.

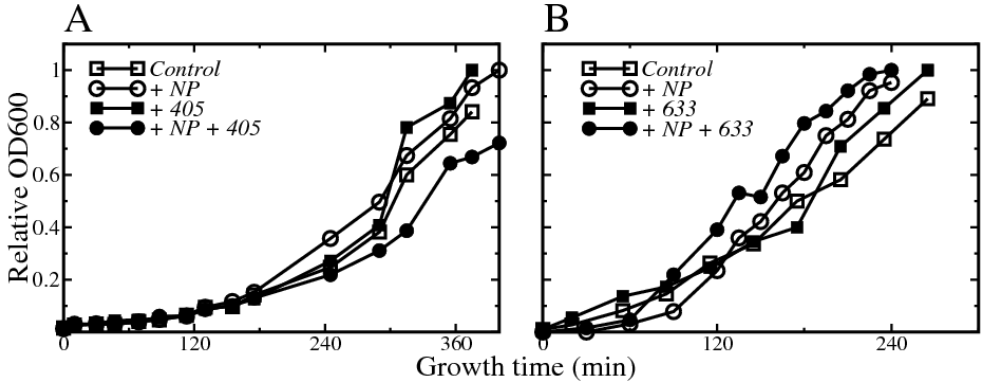


**Figure 3.** Bactericidal effects in liquid media. *E. coli* growing curves represented as the variation in OD600 (normalized with respect to the maximum growth) versus time under different treatments. A concentration of $6.5x10^{14}$ NP $L^{-1}$ was used in all cases. (A) Samples grown with irradiation using the blue laser (405 nm, filled symbols) or without irradiation (empty symbols), either in presence (circles) or absence (squares) of Ag@silica NP. (B) Samples grown with irradiation using the red laser (633 nm, filled symbols) or without irradiation (empty symbols), either in presence (circles) or absence (squares) of Ag@silica NP.

However, the experiments in liquid cultures do not inform about effects on cell viability since they do not allow distinguishing between a reduction of the cell division rate and a reduction of the number of viable cells. Additionally, we have a poor control of the effective irradiation time because we can only affect a fraction of the total volume, where the population of cells is changing with time due to the movement of bacteria within the entire sample. Thus, we used an alternative setup consisting on the irradiation of solid cultures, for which bacterial diffusion is limited and we can assume constant irradiation conditions over the population of bacteria under the laser spot. As a solid medium we used LB-agar plates, onto which bacteria were spread and allowed to grow forming colonies which ideally should cover the complete surface. Ag@silica NP were present at a concentration of 6.5 $x10^{14}$ NP $L^{-1}$ in both, the liquid culture used to inoculate the plates and the LB-agar medium, and irradiations with the blue and the red lasers were maintained during the complete growth and performed over selected, constant, non overlapping small areas of the same plate. Figure 4 shows enlarged areas of the plates after 16 hours of growing (time needed for a normal development of colonies) with continuous irradiation with the blue laser, and in presence or absence of Ag@silica NP. In the images, white color corresponds to the agar surface covered with *E. coli* colonies, dark gray spots are free from bacteria. The zones irradiated with the blue laser are indicated with an arrow. In the plate without NP (figure 4B) this irradiated area is covered with colonies and does not distinguish from the background. However, in plates with NP (figures 4A, C and D) the irradiated areas can be clearly seen as a irregular surface free from bacteria with an ellipsoidal shape and dimensions similar to the area of the laser spot (~1.4 $mm^2$). Such zones are not seen under the spot of the red laser, where the irradiated area presents a similar development of colonies as the background (not shown). Moreover, when the blue laser is switched off after a growth with irradiation (in presence of NP, figure 4C), and the plate is kept under optimal growth conditions for

additional 48 hours, the clean region keeps free from *E. coli* colonies (figures 4D), indicating that, in the presence of Ag@silica NP, irradiation with the SPR frequency sterilizes the irradiated area.

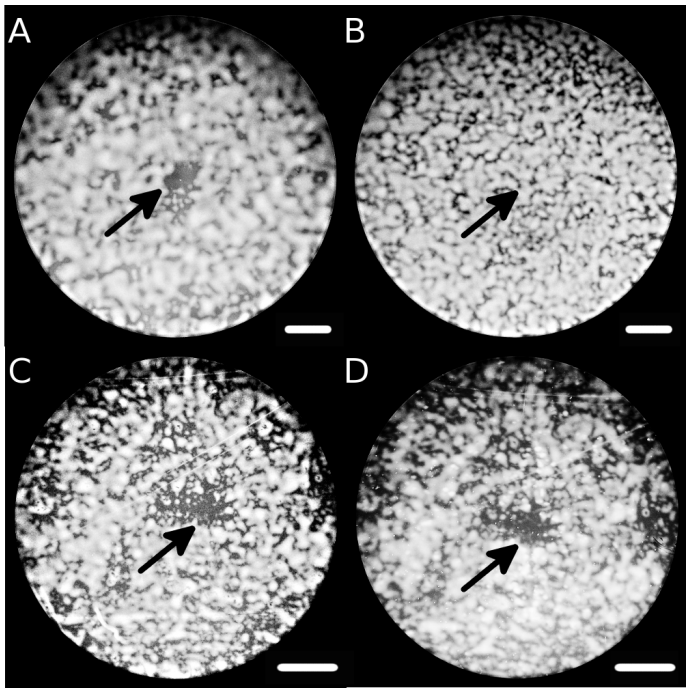


**Figure 4.** Bactericidal effects in solid media. Samples with Ag@silica NP contained $6.5x10^{14}$ NP $L^{-1}$, in both the agar plates and the liquid culture used as inoculum. Enlarged photographs of the Petri dishes were taken after overnight cultures with laser irradiation at zones indicated in the pictures (arrows). (A) Solid culture in presence of Ag@silica NP irradiated with the blue laser (405 nm) near the position marked with the arrow. (B) Same as (A) but without Ag@silica NP. The plates shown in (A) and (B) were also irradiated with the red laser (633 nm) outside the enlarged zone shown here, but the irradiated spot was not distinguishable from the background. (C) Solid culture in medium containing Ag@silica NP irradiated during 16 h at 405 nm near the position marked with the arrow. (D) Same Petri dish as in (C) grown for additional 48h hours without laser irradiation. In all cases the scale bar corresponds to 1.5 mm.

## 4. DISCUSSION

This work illustrates the controllable use of a new type of silica-coated silver NP for bacterial killing, as well as a new application of the SPR phenomenon based on radiation-absorbing metal NP, both suggesting potential biomedical uses for selective elimination of infectious (and possibly also malignant) cells. It is interesting to compare our observations with some recently reported phototherapeutic applications based on metal NP. Outstanding relevance was achieved by proposed cancer treatments through photothermal therapy with gold nanoshells [30,45,46]. These latter experiments are based on a local overheating produced on the irradiated areas due to proximity of the metal NP, which ensures effective absorption of radiation *via* SPR and transfer of energy, in the form of heat, to the surrounding tissue. Hirsh and co-workers observed a temperature increase of about 37ºC over physiological conditions in areas irradiated in the presence of the nanoshells, using a continuous wave diode laser (820 nm) with a power density of 4 W $cm^{-1}$ [45]. This is ~220 times larger than the mean power applied in our case. Although in principle our pulsed blue laser has 2.5-fold larger power at the pulse peak, the excess heat is dissipated during the relatively long periods between pulses, and according to measures by Hockberger et al. using similar conditions the temperature changes during irradiation should be well below 1 ºC [47]. Additionally, it has been shown that hyperthermia-induced photodynamic effects need a surface irradiance dose exceeding 200 mW $cm^{-1}$ [48-52], which is higher than the average power densities used by us here (18 mW $cm^{-1}$). Thus, we conclude that temperature increase during our irradiation experiments must be small and should not have a significant role for our observations. Instead, we hypothesize that the effects described here are due to the plasmon induced at the surface of the Ag@silica NP, which may be able to affect the viability of bacteria.

The exact mechanism of cell killing is not clear at this point, but we can propose a number of possibilities (figure 5). We may first consider a direct attack onto the bacterial surface (the cell wall and/or the plasma membrane) through electromagnetic perturbations due to SPR, thereby affecting the integrity of the membrane barrier (pathway A in figure 5). It is indeed possible to porate cells of different types by applying laser irradiation (optoporation), and this strategy has been used successfully for cell transfection [53-55]. For example, single plant cells can be perforated using 17 ps pulses and one pulse per second of an infrared laser with a pulse power of ~25 kW and a fluence of ~24 J $cm^{-2}$ [55], which corresponds to a power density of ~$14x10^8$ kW $cm^{-2}$. In our case, assuming a light amplification between$10^3$ and $10^4$ fold near the clustered NP bound to *E. coli*, we can estimate a fluence of 70 μJ $cm^{-2}$ and a mean pulse power of ~10 kW being applied over the bacterial surface. This corresponds to a power density of $10^3$ kW $cm^{-2}$, which is five orders of magnitude smaller than the value for poration of plant cells [55]. However, we use 6 times larger pulses and 2 $x10^7$ pulses per second, and the effect is being applied through multiple NP clusters bound on the surface of each cell, which might altogether be enough for producing significant perturbations of the cell barrier.

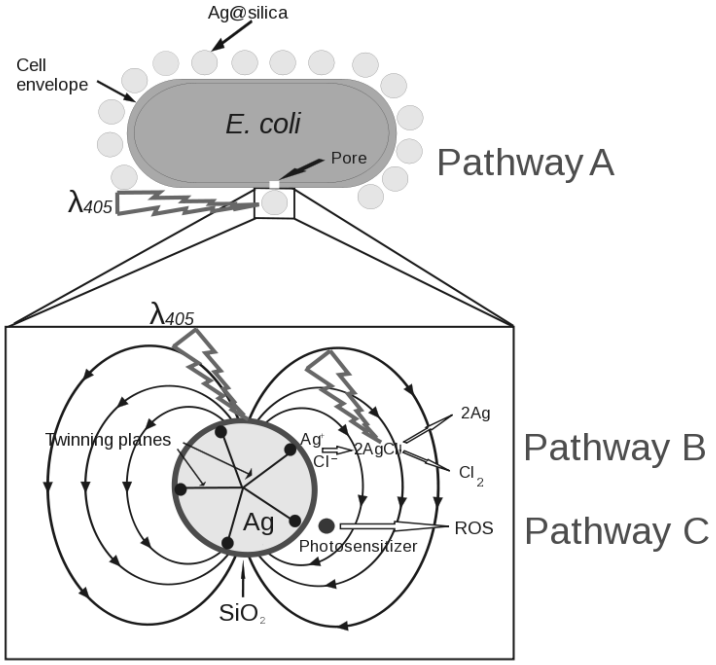


**Figure 5.** Cartoon illustrating possible mechanism of bactericidal effects of Ag@silica NP. Pathway A, Opto-poration: High electromagnetic fields induced by SPR excitation of Ag@silica silver NP would cause intense, localized perturbations at the bacterial cell well and lipid membrane, leading to the formation of pores and compromising the bacterial homeostasis. Pathway B, oxidative-etching: After SPR excitation, and in the presence of chloride ions, the silver in the twin-planes would oxidize and precipitate as AgCl. The high electromagnetic fields induced in the NP surface through SPR would lead to photodissociation of AgCl and the released silver ions would exert a toxic effect on the bacteria. Pathway C, ROS-mediated cell death. Light irradiation, amplified by the plasmonic effect, in the presence of photosensitizers (intrinsic bacterial chromophores) could trigger the formation of highly toxic ROS.

Alternatively, some indirect mechanisms may operate *via* the production of toxic species after irradiation. The first and easiest possibility would be an SPR-dependent formation of $Ag^+$ which might counteract the protective effect of the silica coating (pathway B in figure 5). An enhanced formation of $Ag^+$ cations may occur due to photo-oxidative etching of the silver core of the NP and in presence of $Cl^-$ anions (abundant in the growth medium) [39,40], being the exchange of ions made possible through small pores in the silica shell. Such a reaction is expected to be facilitated in silver NP with a twinned morphology, like the ones used here (see above) because of distortions in the crystal lattice and surface relaxation.

Another possibility would be the photo-oxidative production of toxic reactive oxygen species (ROS) (pathway C in figure 5). These are formed when bacterial endogenous chromophores, such as porphyrins and flavins, absorbing violet light (400-450 nm), are attack by nearby oxygen [47,56-59]. The presence of Ag@silica NP would facilitate an enhancement of the effective light intensity at their surface and a few nanometers beyond, thereby increasing the production of ROS by periplasmic bacterial photosensitizers. Similar combinations of light, a photosensitizer and oxygen active species are used in cancer treatment, normally referred to as photodynamic therapy [60]. Other possible mechanisms may integrate several of the above effects acting synergistically. For instance, electromagnetic perturbations of the cell surface may facilitate the entry of $Ag^+$ cations produced via photooxidative etching, or $Ag^+$ might also contribute to the generation of ROS [61,62].

Recently it has been shown that the antimicrobial effect of silver can be reduced and even removed completely by pre-irradiation with UV light of $Ag/TiO_2$ particles, allowing control of the silver toxicity [23]. The strategy presented here permits a switching control of toxicity using inert Ag@silica NP, where antimicrobial activity can be triggered at will through the specific irradiation using light corresponding to their plasmon absorption band, thus allowing high spatial and temporal resolution.

## 5. CONCLUSIONS

In conclusion, we have developed a new type of silver NP, Ag@silica NP, with three interesting characteristics for biological applications: (1) The NP bind to the *E. coli* cell surface, where they cluster forming NP aggregates. (2) The silica shell stabilizes the colloid reducing the release of silver ions, and the intrinsic toxic effect of the resulting Ag@silicia NP is vanishingly small. (3) Excitation of the Ag@silica NP with light within the SPR band causes inhibition of the growth of *E. coli* in liquid media and sterilization of illuminated areas in solid cultures.

We hypothesize that the surface plasmons originating on the NP are directly or indirectly the cause of the observed photoswitchable cell death. A direct structural effect of the high electromagnetic fields induced through SPR might affect the integrity of the cell barrier. Other likely alternatives include an enhanced ejection of toxic $Ag^+$ cations across the porous silica layer through an SPR-dependent photo-oxidative etching effect, and SPR-induced production of toxic ROS via endogenous chromophores.

## ACKNOWLEDGMENTS

This work has been supported by a grant from the Spanish Ministerio de Ciencia e Innovación (MICINN) (BFU2007-67097), which is financed in part by the European Regional Development Fund (ERDF). EJ thanks MICINN for fellowship of the "Juan de la Cierva" program. GF and OS thank the University of Valencia for "V Segles" and "Invited Researcher" fellowships, respectively.

## REFERENCES

[1] Alivisatos, A.P., "Semiconductor Clusters, Nanocrystals, and Quantum Dots," Science 271(5251), 933-937 (1996).
[2] Hutter, E., and Fendler, J.H., "Exploitation of Localized Surface Plasmon Resonance," Adv Marter 16(19), 1685-1706 (2004).
[3] Sondi, I., and Salopek-Sondi, B., "Silver nanoparticles as antimicrobial agent: a case study on E. coli as a model for Gram-negative bacteria," J Colloid Interface Sci 275(1), 177-82 (2004).
[4] Stoimenov, P.K., Klinger, R.L., Marchin, G.L., and Klabunde, K.J., "Metal Oxide Nanoparticles as Bactericidal Agents," Langmuir 18(17), 6679-6686 (2002).
[5] Beggs, C.B., Noakes, C.J., Sleigh, P.A., Fletcher, L.A., and Kerr, K.G., "Methodology for determining the susceptibility of airborne microorganisms to irradiation by an upper-room UVGI system," J Aerosol Sci 37(7), 885-902 (2006).

[6] Zhao, G.J., and Stevens, S.E., "Multiple parameters for the comprehensive evaluation of the susceptibility of Escherichia coli to the silver ion," Biometals 11(1), 27-32 (1998).
[7] Hsiao, M.T., Chen, S.F., Shieh, D.B., and Yeh, C.S., "One-Pot Synthesis of Hollow Au3Cu1 Spherical-like and Biomineral Botallackite Cu2(OH)3Cl Flowerlike Architectures Exhibiting Antimicrobial Activity," J Phys Chem B 110(1), 205-210 (2006).
[8] Moyer, C.A., Brentano, L., Gravens, D.L., Margraf, H.W., and Monafo Jr., W.W., "Treatment of Large Human Burns with 0.5 Per Cent Silver Nitrate Solution," Arch Surg 90, 812-67 (1965).
[9] Hoopes, J.E., Butcher Jr., H.R., Margraf, H.W., and Gravens, D.L., "Silver lactate burn cream," Surgery 70(1), 29-37 (1971).
[10] Fox Jr., C.L., Rappole, B.W., and Stanford, W., "Control of pseudomonas infection in burns by silver sulfadiazine," Surg Gynecol Obstet 128(5), 1021-6 (1969).
[11] Yoshida, K., Tanagawa, M., Matsumoto, S., Yamada, T., and Atsuta, M., "Antibacterial activity of resin composites with silver-containing materials," Eur J Oral Sci 107(4), 290-6 (1999).
[12] Bosetti, M., Masse, A., Tobin, E., and Cannas, M., "Silver coated materials for external fixation devices: in vitro biocompatibility and genotoxicity," Biomaterials 23(3), 887-92 (2002).
[13] Samuel, U., and Guggenbichler, J.P., "Prevention of catheter-related infections: the potential of a new nano-silver impregnated catheter," Int J Antimicrob Agents 23 Suppl 1, S75-8 (2004).
[14] Lok, C.N., Ho, C.M., Chen, R., He, Q.Y., Yu, W.Y., Sun, H., Tam, P.K., Chiu, J.F., and Che, C.M., "Proteomic analysis of the mode of antibacterial action of silver nanoparticles," J Proteome Res 5(4), 916-24 (2006).
[15] Hwang, E.T., Lee, J.H., Chae, Y.J., Kim, Y.S., Kim, B.C., Sang, B.-I., and Gu, M.B., "Analysis of the toxic mode of action of silver nanoparticles using stress-specific bioluminescent bacteria," Small 4(6), 746-50 (2008).
[16] Jeon, H.-J., Yi, S.-C., and Oh, S.-G., "Preparation and antibacterial effects of Ag-SiO2 thin films by sol-gel method," Biomaterials 24(27), 4921-4928 (2003).
[17] Dibrov, P., Dzioba, J., Gosink, K.K., and Hase, C.C., "Chemiosmotic mechanism of antimicrobial activity of Ag(+) in Vibrio cholerae," Antimicrob Agents Chemother 46(8), 2668-70 (2002).
[18] Nel, A., Xia, T., Mädler, L., and Li, N., "Toxic potential of materials at the nanolevel," Science 311(5761), 622-7 (2006).
[19] Yoon, K.Y., Byeon, J.H., Park, J.H., and Hwang, J., "Susceptibility constants of Escherichia coli and Bacillus subtilis to silver and copper nanoparticles," Sci Total Environ 373(2-3), 572-5 (2007).
[20] Thiel, J., Pakstis, L., Buzby, S., Raffi, M., Ni, C., Pochan, D.J., and Shah, S.I., "Antibacterial properties of silver-doped titania," Small 3(5), 799-803 (2007).
[21] Park, S.J., and Jang, Y.S., "Preparation and characterization of activated carbon fibers supported with silver metal for antibacterial behavior," J Colloid Interface Sci 261(2), 238-243 (2003).
[22] Morrison, M.L., Buchanan, R.A., Liaw, P.K., Berry, C.J., Brigmon, R.L., Riester, L., Abernathy, H., Jin, C., and Narayan, R.J., "Electrochemical and antimicrobial properties of diamondlike carbon-metal composite films," Diam Relat Mater 15(1), 138-146 (2006).
[23] Gunawan, C., Teoh, W.Y., Marquis, C.P., Lifia, J., and Amal, R., "Reversible Antimicrobial Photoswitching in Nanosilver," Small (2009).
[24] Jeanmaire, D.L., and Duyne, R.P.V., "Surface raman spectroelectrochemistry: Part I. Heterocyclic, aromatic, and aliphatic amines adsorbed on the anodized silver electrode," J Electroanal Chem 84(1), 1-20 (1977).
[25] Nie, S., and Emory, S.R., "Probing Single Molecules and Single Nanoparticles by Surface-Enhanced Raman Scattering," Science 275(5303), 1102-1106 (1997).
[26] Kneipp, K., Wang, Y., Kneipp, H., Perelman, L.T., Itzkan, I., Dasari, R.R., and Feld, M.S., "Single Molecule Detection Using Surface-Enhanced Raman Scattering (SERS)," Phys Rev Lett 78(9), 1667-1667 (1997).
[27] Moskovits, M., "Surface roughness and the enhanced intensity of Raman scattering by molecules adsorbed on metals," J Chem Phys 69(9), 4159-4161 (1978).
[28] Gersten, J., and Nitzan, A., "Electromagnetic theory of enhanced Raman scattering by molecules adsorbed on rough surfaces," J Chem Phys 73(7), 3023-3037 (1980).
[29] Homola, J., "Present and future of surface plasmon resonance biosensors," Anal Bioanal Chem 377(3), 528-39 (2003).
[30] O'Neal, D.P., Hirsch, L.R., Halas, N.J., Payne, J.D., and West, J.L., "Photo-thermal tumor ablation in mice using near infrared-absorbing nanoparticles," Cancer Lett 209(2), 171-176 (2004).

[31] Maier, S.A., Kik, P.G., Atwater, H.A., Meltzer, S., Harel, E., Koel, B.E., and Requicha, A.A., "Local detection of electromagnetic energy transport below the diffraction limit in metal nanoparticle plasmon waveguides," Nature Mater 2(4), 229-232 (2003).
[32] Zhang, J., Li, X., Sun, X., and Li, Y., "Surface Enhanced Raman Scattering Effects of Silver Colloids with Different Shapes," J Phys Chem B 109(25), 12544-12548 (2005).
[33] Li, K., Stockman, M.I., and Bergman, D.J., "Self-similar chain of metal nanospheres as an efficient nanolens," Phys Rev Lett 91(22), 227402 (2003).
[34] Sweatlock, L.A., Maier, S.A., Atwater, H.A., Penninkhof, J.J., and Polman, A., "Highly confined electromagnetic fields in arrays of strongly coupled Ag nanoparticles," Phys Rev B Condens Matter Mater Phys 71(23), 235408-7 (2005).
[35] Käll, M., Xu, H., and Johansson, P., "Field enhancement and molecular response in surface-enhanced Raman scattering and fluorescence spectroscopy," Journal of Raman Spectroscopy 36(6-7), 510-514 (2005).
[36] Kamat, P.V., Flumiani, M., and Hartland, G.V., "Picosecond Dynamics of Silver Nanoclusters. Photoejection of Electrons and Fragmentation," J Phys Chem B 102(17), 3123-3128 (1998).
[37] Kurita, H., Takami, A., and Koda, S., "Size reduction of gold particles in aqueous solution by pulsed laser irradiation," Appl Phys Lett 72(7), 789-791 (1998).
[38] Takami, A., Kurita, H., and Koda, S., "Laser-Induced Size Reduction of Noble Metal Particles," J Phys Chem B 103(8), 1226-1232 (1999).
[39] Wiley, B., Herricks, T., Sun, Y., and Xia, Y., "Polyol Synthesis of Silver Nanoparticles: Use of Chloride and Oxygen to Promote the Formation of Single-Crystal, Truncated Cubes and Tetrahedrons," Nano Lett 4(9), 1733-1739 (2004).
[40] Tsuji, T., Okazaki, Y., Higuchi, T., and Tsuji, M., "Laser-induced morphology changes of silver colloids prepared by laser ablation in water: Enhancement of anisotropic shape conversions by chloride ions," J Photochem Photobiol A 183(3), 297-303 (2006).
[41] Jin, R., Cao, Y., Mirkin, C.A., Kelly, K.L., Schatz, G.C., and Zheng, J.G., "Photoinduced Conversion of Silver Nanospheres to Nanoprisms," Science 294(5548), 1901-1903 (2001).
[42] Jin, R., Cao, Y.C., Hao, E., Metraux, G.S., Schatz, G.C., and Mirkin, C.A., "Controlling anisotropic nanoparticle growth through plasmon excitation," Nature 425(6957), 487-490 (2003).
[43] Jiménez, E., Abderrafi, K., Martínez-Pastor, J., Abargues, R., Luís Valdés, J., and Ibáñez, R., "A novel method of nanocrystal fabrication based on laser ablation in liquid environment," Superlattices Microstruct 43(5-6), 487-493 (2008).
[44] Jiménez, E., Abderrafi, K., Abargues, R., Valdés, J.L., and Martínez-Pastor, J.P., "Laser-ablation-induced synthesis of SiO2-capped noble metal nanoparticles in a single step," Langmuir: The ACS Journal of Surfaces and Colloids 26(10), 7458-7463 (2010).
[45] Hirsch, L.R., Stafford, R.J., Bankson, J.A., Sershen, S.R., Rivera, B., Price, R.E., Hazle, J.D., Halas, N.J., and West, J.L., "Nanoshell-mediated near-infrared thermal therapy of tumors under magnetic resonance guidance," Proc Natl Acad Sci USA 100(23), 13549-13554 (2003).
[46] Choi, M.-R., Stanton-Maxey, K.J., Stanley, J.K., Levin, C.S., Bardhan, R., Akin, D., Badve, S., Sturgis, J., Robinson, J.P., et al., "A Cellular Trojan Horse for Delivery of Therapeutic Nanoparticles into Tumors," Nano Lett 7(12), 3759-3765 (2007).
[47] Hockberger, P.E., Skimina, T.A., Centonze, V.E., Lavin, C., Chu, S., Dadras, S., Reddy, J.K., and White, J.G., "Activation of flavin-containing oxidases underlies light-induced production of H2O2 in mammalian cells," Proc Natl Acad Sci USA 96(11), 6255-6260 (1999).
[48] Svaasand, L.O., "Photodynamic and photohyperthermic response of malignant tumors," Med Phys 12(4), 455-461 (1985).
[49] Henderson, B.W., Waldow, S.M., Potter, W.R., and Dougherty, T.J., "Interaction of photodynamic therapy and hyperthermia: tumor response and cell survival studies after treatment of mice in vivo," Cancer Res 45(12 Pt 1), 6071-6077 (1985).
[50] Levendag, P.C., Marijnissen, H.P., Ru, V.J. de, Versteeg, J.A., Rhoon, G.C. van, and Star, W.M., "Interaction of interstitial photodynamic therapy and interstitial hyperthermia in a rat rhabdomyosarcoma--a pilot study," Int J Radiat Oncol Biol Phys 14(1), 139-145 (1988).
[51] Leunig, M., Leunig, A., Lankes, P., and Goetz, A.E., "Evaluation of photodynamic therapy-induced heating of hamster melanoma and its effect on local tumour eradication," Int J Hyperthermia 10(2), 297-306 (1994).

[52] Marijnissen, J.P., Baas, P., Beek, J.F., Moll, J.H. van, Zandwijk, N. van, and Star, W.M., "Pilot study on light dosimetry for endobronchial photodynamic therapy," Photochem Photobiol 58(1), 92-99 (1993).
[53] Tao, W., Wilkinson, J., Stanbridge, E.J., and Berns, M.W., "Direct Gene Transfer into Human Cultured Cells Facilitated by Laser Micropuncture of the Cell Membrane," Proc Natl Acad Sci USA 84(12), 4180-4184 (1987).
[54] Tirlapur, U.K., and Konig, K., "Cell biology: Targeted transfection by femtosecond laser," Nature 418(6895), 290-291 (2002).
[55] Schinkel, H., Jacobs, P., Schillberg, S., and Wehner, M., "Infrared picosecond laser for perforation of single plant cells," Biotechnol Bioeng 99(1), 244-248 (2008).
[56] Pal, G., Dutta, A., Mitra, K., Grace, M.S., Amat, A., Romanczyk, T.B., Wu, X., Chakrabarti, K., Anders, J., et al., "Effect of low intensity laser interaction with human skin fibroblast cells using fiber-optic nano-probes," J Photochem Photobiol B 86(3), 252-261 (2007).
[57] Kale, H., Harikumar, P., Kulkarni, S.B., Nair, P.M., and Netrawali, M.S., "Assessment of the genotoxic potential of riboflavin and lumiflavin. B. Effect of light," Mutat Res 298(1), 17-23 (1992).
[58] Edwards, A.M., and Silva, E., "Effect of visible light on selected enzymes, vitamins and amino acids," J Photochem Photobiol B 63(1-3), 126-131 (2001).
[59] Kearns, D.R., "Physical and chemical properties of singlet molecular oxygen," Chem Rev 71(4), 395-427 (1971).
[60] Dougherty, T.J., Gomer, C.J., Henderson, B.W., Jori, G., Kessel, D., Korbelik, M., Moan, J., and Peng, Q., "Photodynamic therapy," J Natl Cancer Inst 90(12), 889-905 (1998).
[61] Hussain, S.M., Hess, K.L., Gearhart, J.M., Geiss, K.T., and Schlager, J.J., "In vitro toxicity of nanoparticles in BRL 3A rat liver cells," Toxicol In Vitro 19(7), 975-83 (2005).
[62] Yoshimaru, T., Suzuki, Y., Inoue, T., Niide, O., and Ra, C., "Silver activates mast cells through reactive oxygen species production and a thiol-sensitive store-independent Ca2+ influx," Free Radic Biol Med 40(11), 1949-59 (2006).